Higher-Order Convolution PML (CPML) for FDTD electromagnetic modelling

Higher-Order Convolution PML (CPML) for FDTD electromagnetic modelling

Antonios Giannopoulos

***Abstract*—A new simple formulation for incorporating a higher-order perfectly matched layer (PML) stretching function within a convolution PML (CPML) implementation in finite-difference time-domain (FDTD) electromagnetic modelling codes is developed. Obtaining in closed form the corresponding time domain impulse response of the inverse of a number of higher-order PML stretching functions enables the efficient and simple implementation of such higher-order PMLs using recursive convolution, in the same way as it was introduced initially for the complex frequency shifted (CFS) PML. This new higher-order CPML exhibits excellent performance that is comparable to the performance shown by other higher-order PML formulations whilst it retains the advantage of a relatively simpler implementation.**

***Index Terms*—Absorbing Boundary Conditions, Finite Difference Methods, Perfectly Matched Layer, Recursive Convolution, FDTD, PML**

I. Introduction

ONE of the most successful and popular PML implementations used in FDTD [1], [2] is the Convolution PML as introduced by Roden and Gedney [3]. Some of the reasons for the popularity of the CPML are that it is media agnostic, as it is based on a stretched co-ordinate PML formulation [4], [5], and that the use of a direct implementation in the time domain of a recursive convolution results in a rather simple and efficient implementation. The key design idea behind the CPML approach is the exploitation of an efficient scheme for performing a recursive convolution in the time domain, firstly introduced in mainstream FDTD modelling for incorporating frequency dispersive materials [6]. To implement such an approach the impulse response of the inverse of the PML's stretching function, defined in the frequency domain, should be available in closed form and specified primarily via an exponential function. For a standard (i.e. a single) CFS pole a relatively simple closed form expression for the required impulse response is easily derived and this has been the basis for the CPML formulation as was presented for the first time in [3]. A trapezoidal recursive convolution (TRC) scheme was used by default, mainly due to the arrangement of the field components involved in the convolution integral which ensured that CPML is a second order accurate numerical scheme [7] as is the main FDTD algorithm. Obviously, it is the exponential nature of the time domain impulse response that allowed for the recursive evaluation of the otherwise computationally demanding convolution integrals.

A. Giannopoulos is with the School of Engineering, Institute for Infrastructure and Environment, The University of Edinburgh, EH9 3FG, UK e-mail: (A.Giannopoulos@ed.ac.uk)

Manuscript received January 14, 2020; accepted March 30, 2020

For a number of FDTD modelling problems it has been shown that a second order PML stretching function can improve the performance of the PML absorbing region as demonstrated by Correia and Jin who introduced the idea and the first such PML formulation [8] and soon after showcased the improvement in performance [9]. Subsequently, a number of PML formulations have been developed to accommodate such more complex stretching functions [10]–[13]. Until now, however, it appears that no attempt has been reported in the literature, to apply directly the design idea that has led to the original CPML approach, in implementing a higher-order PML. This possibly could be due to the increase in complexity and tediousness in obtaining the impulse response of higher-order PML stretching functions in closed form. An attempt however, to use the CPML approach for a 2nd order PML has been reported in [14] but this was based on what appears to be the creation of a system of interdependent simpler first order recursive convolutions. Although the attempt appeared to perform well, the authors reported stability issues and they did resort to recommending restricting the range of PML parameters. No further development of this approach has been presented or followed further.

In this paper, first, a general formula in closed form for the impulse response of the inverse of higher-order PML stretching functions is presented, and then used to implement in FDTD a higher-order PML using the CPML approach. It will be shown that the resulting formulation retains the simplicity of the original CPML, is numerically efficient and can be easily introduced in FDTD codes that already implement the standard CPML with minimum effort.

II. Theory

Maxwell's equations in frequency domain and in stretched co-ordinates can be presented compactly as

$$\jmath\omega\tilde{D}_i = \frac{1}{s_j}\frac{\partial\tilde{H}_k}{\partial j} - \frac{1}{s_k}\frac{\partial\tilde{H}_j}{\partial k} \tag{1}$$

$$\jmath\omega\tilde{B}_i = \frac{1}{s_k}\frac{\partial\tilde{E}_j}{\partial k} - \frac{1}{s_j}\frac{\partial\tilde{E}_k}{\partial j} \tag{2}$$

using the cyclic notation $(i,j,k) \in (x,y,z),(y,z,x),(z,x,y)$, where s_u with $u \in (i,j,k)$ is a higher-order PML stretching function defined by

$$s_u = \prod_{m=1}^{M} (\kappa_{u_m} + \frac{\sigma_{u_m}}{\alpha_{u_m} + \jmath\omega\epsilon_0}) \tag{3}$$

where M is the number of general CFS poles that make up the higher-order stretching function and its individual terms are of

the general form presented originally in [15]. Using $\bar{s} = s^{-1}$ and converting to time domain

$$\frac{\partial D_i}{\partial t} = \bar{s}_j(t) \star \frac{\partial H_k}{\partial j} - \bar{s}_k(t) \star \frac{\partial H_j}{\partial k} \tag{4}$$

$$\frac{\partial B_i}{\partial t} = \bar{s}_k(t) \star \frac{\partial E_j}{\partial k} - \bar{s}_j(t) \star \frac{\partial E_k}{\partial j} \tag{5}$$

It has been shown in [3] that for $M = 1$, for which (3) reduces to the standard CFS-PML stretching function, $\bar{s}_u(t)$ is

$$\bar{s}_u(t) = \frac{\delta(t)}{\kappa_u} - \frac{\sigma_u e^{-t(\frac{\alpha_u \kappa_u + \sigma_u}{\epsilon_0 \kappa_u})}}{\epsilon_0 \kappa_u^2} u(t) \tag{6}$$

where $\delta(t)$ and $u(t)$ are the Dirac delta and the Heaviside step functions respectively. Using Laplace transforms, and although not formally proven for all positive M, it has been verified with the help of a computer algebra program [16] that for up to at least $M = 10$ the impulse response of $1/s_u$ with a PML stretching function, as defined in (3), takes the general form

$$\begin{aligned} \bar{s}_u(t) = & \frac{\delta(t)}{\prod_{m=1}^{M} \kappa_{u_m}} \\ & - \frac{1}{\epsilon_0} \sum_{m=1}^{M} e^{-t(\frac{\alpha_{u_m} \kappa_{u_m} + \sigma_{u_m}}{\epsilon_0 \kappa_{u_m}})} \frac{\sigma_{u_m} \prod_{\substack{l=1 \\ l \neq m}}^{M} \Lambda_{u_{m,l}}}{\kappa_{u_m}^2 \prod_{\substack{l=1 \\ l \neq m}}^{M} \Xi_{u_{m,l}}} u(t) \end{aligned} \tag{7}$$

where the following are introduced to simplify the presentation and $m, l \in (1 \dots M)$ with $l \neq m$

$$\begin{aligned} \Lambda_{u_{m,l}} &= \alpha_{u_m} \kappa_{u_m} - \alpha_{u_l} \kappa_{u_m} + \sigma_{u_m} \\ \Xi_{u_{m,l}} &= \alpha_{u_m} \kappa_{u_m} \kappa_{u_l} - \alpha_{u_l} \kappa_{u_m} \kappa_{u_l} + \kappa_{u_l} \sigma_{u_m} - \kappa_{u_m} \sigma_{u_l} \end{aligned} \tag{8}$$

The case of interest here and for most practical applications is when $M = 2$ and the PML stretching function takes a form that has been shown that it can improve performance [8] for some FDTD modelling problems. The impulse response for $M = 2$ obtained easily from (7) is

$$\begin{aligned} \bar{s}_u(t) = & \frac{\delta(t)}{\kappa_{u_1} \kappa_{u_2}} - \frac{e^{-t(\frac{\alpha_{u_1} \kappa_{u_1} + \sigma_{u_1}}{\epsilon_0 \kappa_{u_1}})} \sigma_{u_1} \Lambda_{u_{1,2}} u(t)}{\epsilon_0 \kappa_{u_1}^2 \Xi_{u_{1,2}}} \\ & - \frac{e^{-t(\frac{\alpha_{u_2} \kappa_{u_2} + \sigma_{u_2}}{\epsilon_0 \kappa_{u_2}})} \sigma_{u_2} \Lambda_{u_{2,1}} u(t)}{\epsilon_0 \kappa_{u_2}^2 \Xi_{u_{2,1}}} \end{aligned} \tag{9}$$

Introducing (9) into (4), to apply the CPML concept as presented in [3], results in

$$\frac{\partial D_i}{\partial t} = \frac{1}{\kappa_{j_1} \kappa_{j_2}} \frac{\partial H_k}{\partial j} + \zeta_j(t) \star \frac{\partial H_k}{\partial j} - \frac{1}{\kappa_{k_1} \kappa_{k_2}} \frac{\partial H_j}{\partial k} - \zeta_k(t) \star \frac{\partial H_j}{\partial k} \tag{10}$$

where

$$\begin{aligned} \zeta_u(t) = & - \frac{e^{-t(\frac{\alpha_{u_1} \kappa_{u_1} + \sigma_{u_1}}{\epsilon_0 \kappa_{u_1}})} \sigma_{u_1} \Lambda_{u_{1,2}} u(t)}{\epsilon_0 \kappa_{u_1}^2 \Xi_{u_{1,2}}} \\ & - \frac{e^{-t(\frac{\alpha_{u_2} \kappa_{u_2} + \sigma_{u_2}}{\epsilon_0 \kappa_{u_2}})} \sigma_{u_2} \Lambda_{u_{2,1}} u(t)}{\epsilon_0 \kappa_{u_2}^2 \Xi_{u_{2,1}}} \end{aligned} \tag{11}$$

defining the discrete impulse response as

$$\begin{aligned} Z_{0_u}(q) = & \int_{q\Delta t}^{(q+1)\Delta t} \zeta_u(\tau) d\tau \\ = & - \frac{\sigma_{u_1} \Lambda_{u_{1,2}}}{\epsilon_0 \kappa_{u_1}^2 \Xi_{u_{1,2}}} \int_{q\Delta t}^{(q+1)\Delta t} e^{-\tau(\frac{\alpha_{u_1} \kappa_{u_1} + \sigma_{u_1}}{\epsilon_0 \kappa_{u_1}})} d\tau \\ & - \frac{\sigma_{u_2} \Lambda_{u_{2,1}}}{\epsilon_0 \kappa_{u_2}^2 \Xi_{u_{2,1}}} \int_{q\Delta t}^{(q+1)\Delta t} e^{-\tau(\frac{\alpha_{u_2} \kappa_{u_2} + \sigma_{u_2}}{\epsilon_0 \kappa_{u_2}})} d\tau \end{aligned} \tag{12}$$

can arrive at

$$Z_{0_u}(q) = a_{u_1} e^{-q\Delta t(\frac{\alpha_{u_1} \kappa_{u_1} + \sigma_{u_1}}{\epsilon_0 \kappa_{u_1}})} + a_{u_2} e^{-q\Delta t(\frac{\alpha_{u_2} \kappa_{u_2} + \sigma_{u_2}}{\epsilon_0 \kappa_{u_2}})} \tag{13}$$

where a_{u_1} and a_{u_2} are defined as

$$a_{u_1} = \frac{\sigma_{u_1} \Lambda_{u_{1,2}}}{\kappa_{u_1}(\alpha_{u_1} \kappa_{u_1} + \sigma_{u_1}) \Xi_{u_{1,2}}} \left(e^{-\Delta t(\frac{\alpha_{u_1} \kappa_{u_1} + \sigma_{u_1}}{\epsilon_0 \kappa_{u_1}})} - 1 \right) \tag{14}$$

$$a_{u_2} = \frac{\sigma_{u_2} \Lambda_{u_{2,1}}}{\kappa_{u_2}(\alpha_{u_2} \kappa_{u_2} + \sigma_{u_2}) \Xi_{u_{2,1}}} \left(e^{-\Delta t(\frac{\alpha_{u_2} \kappa_{u_2} + \sigma_{u_2}}{\epsilon_0 \kappa_{u_2}})} - 1 \right) \tag{15}$$

The general form of an FDTD update of (10) can then be constructed

$$\begin{aligned} & \frac{D_{i_{i+1/2,j,k}}^{n+1} - D_{i_{i+1/2,j,k}}^{n}}{\Delta t} = \\ & \frac{1}{\kappa_{j_1} \kappa_{j_2}} \frac{H_{k_{i+1/2,j+1/2,k}}^{n+1/2} - H_{k_{i+1/2,j-1/2,k}}^{n+1/2}}{\Delta j} + \\ & \sum_{q=0}^{N} Z_{0_j}(q) \frac{H_{k_{i+1/2,j+1/2,k}}^{n-q+1/2} - H_{k_{i+1/2,j-1/2,k}}^{n-q+1/2}}{\Delta j} \\ & - \frac{1}{\kappa_{k_1} \kappa_{k_2}} \frac{H_{j_{i+1/2,j,k+1/2}}^{n+1/2} - H_{j_{i+1/2,j,k-1/2}}^{n+1/2}}{\Delta k} - \\ & \sum_{q=0}^{N} Z_{0_k}(q) \frac{H_{j_{i+1/2,j,k+1/2}}^{n-q+1/2} - H_{j_{i+1/2,j,k-1/2}}^{n-q+1/2}}{\Delta k} \end{aligned} \tag{16}$$

that can be simply written as

$$\begin{aligned} & \frac{D_{i_{i+1/2,j,k}}^{n+1} - D_{i_{i+1/2,j,k}}^{n}}{\Delta t} = \\ & \frac{1}{\kappa_{j_1} \kappa_{j_2}} \frac{H_{k_{i+1/2,j+1/2,k}}^{n+1/2} - H_{k_{i+1/2,j-1/2,k}}^{n+1/2}}{\Delta j} + \psi_{D_{ij_1}}^{n+1} + \psi_{D_{ij_2}}^{n+1} \\ & - \frac{1}{\kappa_{k_1} \kappa_{k_2}} \frac{H_{j_{i+1/2,j,k+1/2}}^{n+1/2} - H_{j_{i+1/2,j,k-1/2}}^{n+1/2}}{\Delta k} - \psi_{D_{ik_1}}^{n+1} - \psi_{D_{ik_2}}^{n+1} \end{aligned} \tag{17}$$

introducing the $\psi_{D_{iu_m}}$ CPML memory variables that conveniently allow us to compute recursively and efficiently the

discrete convolutions in (16) and are simply updated using

$$\psi^{n+1}_{D_{iu_1}} = b_{u_1}\psi^{n}_{D_{iu_1}} + a_{u_1}\frac{H^{n+1/2}_{j_{i+1/2,j,k+1/2}} - H^{n+1/2}_{j_{i+1/2,j,k-1/2}}}{\Delta k} \tag{18}$$

$$\psi^{n+1}_{D_{iu_2}} = b_{u_2}\psi^{n}_{D_{iu_2}} + a_{u_2}\frac{H^{n+1/2}_{j_{i+1/2,j,k+1/2}} - H^{n+1/2}_{j_{i+1/2,j,k-1/2}}}{\Delta k} \tag{19}$$

with

$$b_{u_1} = e^{-\Delta t(\frac{\alpha_{u_1}\kappa_{u_1}+\sigma_{u_1}}{\epsilon_0\kappa_{u_1}})} \text{ and } b_{u_2} = e^{-\Delta t(\frac{\alpha_{u_2}\kappa_{u_2}+\sigma_{u_2}}{\epsilon_0\kappa_{u_2}})} \tag{20}$$

It is important to state that it has not yet been shown that such a PML stretching function of order higher than 2 improves the performance to a level that justifies the extra computational resource required to implement it. However, a 3rd order PML was implemented, tried and tested to further verify the validity of (7) and of the approach. However, its performance was found to be about the same as an optimised 2nd order PML.

In terms of stability it is important to note that for any PML the following conditions should be satisfied [11]

$$\Re(s_u) \geq 1 \text{ and } \Im(s_u) > 0 \tag{21}$$

however, in higher-order PMLs these conditions can become more cumbersome to verify. For a 2nd order PML that is built using the product of a standard PML stretching function (i.e. $\alpha_1 = 0$) and of a CFS-PML one, as presented in [8], using $\alpha_2 > \sigma_1$ and $\kappa_2 \geq 1$ ensures that the conditions in (21) are satisfied for all frequencies [11]. Extensive numerical tests have been carried out for the 2nd order CPML presented here and have not indicated any stability problems that require any other different restrictions imposed for its application.

Another aspect to be highlighted is the fact that the CPML memory variables are not in exact time synchronisation with the rest of the FDTD update equations [17, pp. 66], [7]. This is evident by examining (17) as the equation is time centred at the $n + 1/2$ instance whereas the PML memory variables that are used represent the values of the discrete convolutions at $n+1$. This is easy to rectify as shown in [7] but the CPML does work well without such synchronisation as pointed out in [17, pp. 66] and is supported by the results obtained here.

III. Numerical Results

To demonstrate the effectiveness and performance of the higher-order CPML presented here numerical examples are used that have been employed previously [11], in assessing other similar higher-order PML formulations. This way, a better comparison can be made between approaches for implementing higher-order PMLs.

In the following, for building all PMLs used here, σ_{opt} is given by [18]

$$\sigma_{\text{opt}} = \frac{m+1}{150\pi\Delta l} \tag{22}$$

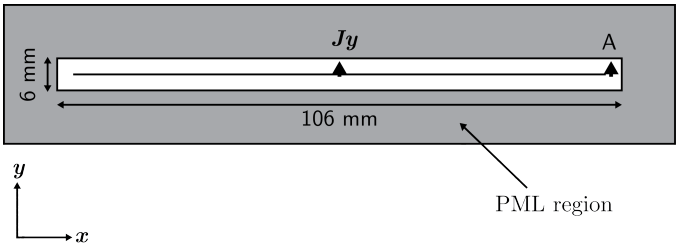

Fig. 1. TE$_z$ FDTD model of a PEC sheet with an electric current source at its centre including a 10-cell thick PML. The E_y field is sampled at point A on the edge of the PEC sheet 3 cells away from the PML boundary.

where m is the order of the relevant polynomial scaling used. Further, in obtaining an estimate of PML errors, at the required testing points, the following formula is used

$$\text{Error}_{\text{db}}|^n_{i,j} = 20\log_{10}\frac{\|E|^n_{i,j} - E_{\text{ref}}|^n_{i,j}\|}{\|E_{\text{ref}_{\text{max}}}|_{i,j}\|} \tag{23}$$

and reference solutions have been obtained using suitably large FDTD models so no appreciable contribution from their truncation boundaries were affecting their solution.

A. Line Source over finite 2D PEC Sheet

A TE$_z$ FDTD grid is used for the 2D numerical test. The model comprises an electric current source oriented in the y direction centred over a perfect electric conductor (PEC) sheet. The current of the source has the following time signature

$$I(t) = -2\frac{(t-t_0)}{t_w}e^{-(\frac{t-t_0}{t_w})^2} \tag{24}$$

where $t_w = 26.53\,\text{ps}$ and $t_0 = 4t_w$. The model, illustrated in Fig. (1), is built using 126×26 1 mm uniform cells and the E_y field component is sampled at A which is placed at the edge of the 100 cell PEC sheet only 3 FDTD cells away from the PML inner boundary which was built using 10 cells. The time step Δt of the simulation was set to be $\Delta t = 0.99\Delta l/c\sqrt{2}$.

Errors from terminating the FDTD grid using a 10-cell standard PML, a CFS-PML, the 2nd order CPML presented here as well as a 2nd order RIPML [11] and a 2nd order CFS-PML as developed in [8] have been calculated. For a standard PML the parameters used were $\sigma = 0.5\sigma_{\text{opt}}$, and $\kappa_{\text{max}} = 8$ employing the same polynomial grading of order $m = 4$ for both. The CFS-PML parameters where obtained from [11] as

$$\kappa = 1 + \kappa_{\text{max}}\Big(\frac{x}{d}\Big)^m$$
$$\sigma = 1.1\sigma_{\text{opt}}\Big(\frac{x}{d}\Big)^m, \;\; \alpha = 0.05$$

where $\kappa_{\text{max}} = 11$ and $m = 4$. d is the thickness of the PML and x is distance from the inner PML interface ($x \in [0, d]$). Similarly, for building the mixed 2nd order CPML

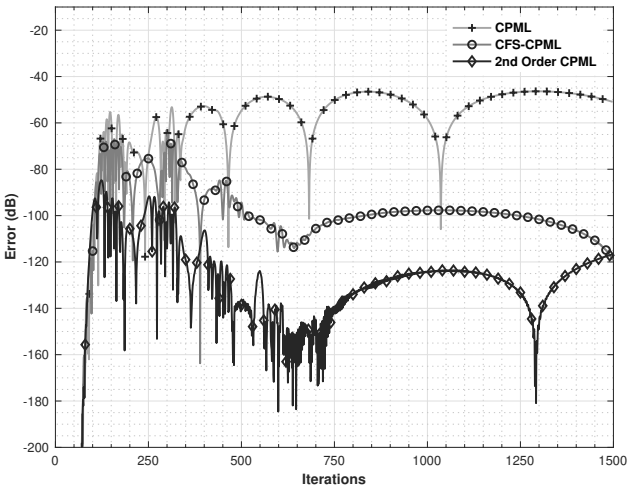

Fig. 2. Errors in the E_y field component at point A for 2D TE$_z$ PEC sheet models terminated using either a 10-cell PML, a CFS-PML, and the new 2nd order CPML.

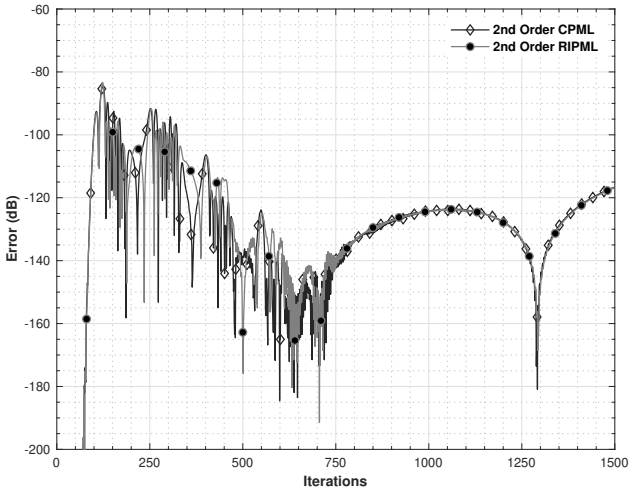

Fig. 3. Errors in the E_y field component at point A for 2D TE$_z$ PEC sheet models terminated using either a 10-cell new 2nd order CPML or a 2nd order RIPML.

its parameters were set to the same ones used to test the RIPML formulation of [11] and were

$$\kappa_1 = 1$$
$$\sigma_1 = \sigma_{1_{\text{opt}}}\left(\frac{x}{d}\right)^6, \quad \alpha_1 = 0$$
$$\kappa_2 = 1 + \kappa_{2_{\text{opt}}}\left(\frac{x}{d}\right)^3$$
$$\sigma_2 = \sigma_{2_{\text{opt}}}\left(\frac{x}{d}\right)^2, \quad \alpha_2 = \alpha_0 + \sigma_1$$

where $\alpha_0 = 0.09$, $\kappa_{2_{\text{opt}}} = 7$, $\sigma_{1_{\text{opt}}} = 0.175/(150\pi\Delta l)$ and $\sigma_{2_{\text{opt}}} = 2.5/(150\pi\Delta l)$

In Fig. (2) the PML errors from the standard PML, CFS-PML and the mixed 2nd order PML using the CPML formulation are presented. It is clear that the new 2nd order CPML performs very well as expected. In Fig. (3) the error obtained using the new CPML 2nd order formulation is compared with the error obtained when using the RIPML [11] and for the same PML parameters. They are clearly very similar, something that does indicate that the absence of exact time synchronisation in the standard CPML does not affect its performance as much as it has shown to do in simple (i.e. first order) PML applications as has been observed in [19] and [7]. To investigate further the small variations between these errors in Fig. (4) the cumulative errors obtained using

$$\text{Error}|_{i,j}^{n} = \sum_{m=1}^{n} \frac{\|E|_{i,j}^{m} - E_{\text{ref}}|_{i,j}^{m}\|}{\|E_{\text{ref}_{\text{max}}}|_{i,j}\|} \tag{25}$$

from the mixed 2nd order PMLs using the new CPML formulation, a time-synchronised version of it following the suggestion of [7], the RIPML of [11] and the first formulation of a higher-order PML as presented by Correia and Jin [8], are presented. What is observed is that the cumulative errors are very close and follow the same pattern. However, it is clear that the errors for the time-synchronised CPML and RIPML are almost identical and similarly almost identical are

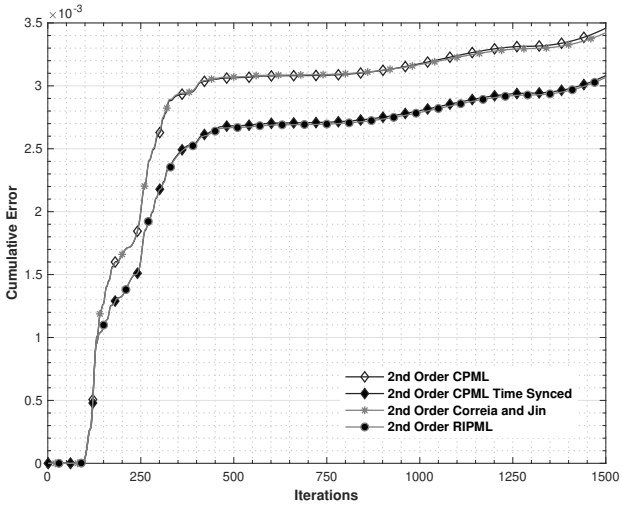

Fig. 4. Cumulative errors, obtained using (25), in the E_y field component at point A for 2D TE$_z$ PEC sheet models terminated using 10-cell 2nd order PMLs using the new CPML, a time-synchronised version of it, RIPML and the formulation of [8].

the errors from the normal CPML and the method presented in by Correia and Jin [8]. Analysing the formulation of Correia and Jin it is clear that it is not time-synchronised either. Although the differences are small the cumulative errors do indicate that a time-synchronised formulation might have a small advantage.

B. Hertzian dipole response from a thin PEC plate

A 3D FDTD model, as illustrated in Fig. (5), of an elongated thin PEC plate has been used to evaluate the performance of the higher-order CPML formulation. The FDTD grid of $51 \times 126 \times 26$ cells [2], used a uniform spatial step of $\Delta l = 1$ mm and a time step $\Delta t = 1.906$ ps. Above the thin plate, having dimensions of 25×100 mm, a z-directed source, with

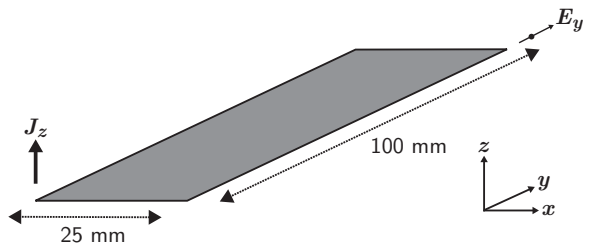

Fig. 5. A z-directed (J_z) electric current dipole source placed 1 mm above the corner of a 25×100 mm thin plate. The E_y field component is sampled 1 mm away from the plate's opposite corner [2].

a time variation as used in the previous 2D example and given by (24), was placed 1 mm above one of the corners of the PEC sheet. The E_y field output was obtained 1 mm away from the diagonally opposite corner. Only three cells separated the edge of the target and the inner surface of the 10-cell thick PMLs. The time-dependent errors calculated using (23) are presented in Fig. (6) for a 10-cell PML, CFS-PML, a 2nd order new CPML and from the 2nd order RIPML [11]. The standard PML parameters where set as $\sigma = 0.7\sigma_{\text{opt}}$, and $\kappa_{\max} = 11$ employing the same polynomial grading of order $m = 4$ for both and the parameters for the CFS-PML where [11]

$$\kappa = 1 + \kappa_{\max}\left(\frac{x}{d}\right)^m$$
$$\sigma = 1.1\sigma_{\text{opt}}\left(\frac{x}{d}\right)^m, \quad \alpha = 0.05$$

where $\kappa_{\max} = 7$ and $m = 4$. Finally, the parameters for the new 2nd order CPML and for RIPML were set as defined for the previous 2D example but with $\sigma_{1_{\text{opt}}} = 0.275/(150\pi\Delta l)$, $\sigma_{2_{\text{opt}}} = 2.75/(150\pi\Delta l)$ and $\alpha_0 = 0.07$ instead [11].

It is evident from Fig. (6) that the new 2nd order CPML formulation improves the performance of the boundary condition in a similar way in the 3D case as it does for the previous 2D case. The performance is very similar to that obtained by RIPML and the errors become practically identical if a time synchronised version of CPML [7] is used.

IV. Conclusion

Although CPML is one of the most popular PML implementations, a simple extension of the original CPML approach to use higher-order PML stretching functions was not, until now, available. Obtaining in closed form the impulse response of the inverse of such higher-order PML stretching functions allowed the application of the recursive convolution approach that resulted in an equally simple process as used for the standard CPML by Roden and Gedney. One key observation that differentiates the higher-order CPML from most of the other higher-order PML formulations is that the updates of the memory variables, supporting the evaluation of the recursive convolutions, are all independent from each other and can be updated in any order. This is not the case in other formulations (e.g. RIPML [11]) where a specific order of updating of the memory variables must be followed. This further simplifies the update of existing FDTD codes, that already use the standard

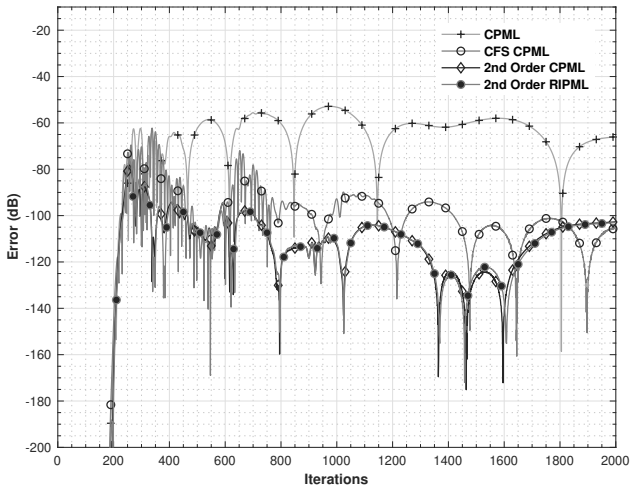

Fig. 6. Errors in the E_y field component obtained one cell away from a PEC thin plate. The FDTD model was terminated using either a 10-cell PML, a CFS-PML, the new 2nd order CPML and a 2nd order RIPML.

CPML, as in addition all memory variable update equations retain the same exact form. Time synchronising the higher-order CPML does not appear to alter greatly its performance but in terms of errors it does make it practically equivalent to the RIPML formulation.

References

[1] K. Yee, "Numerical solution of initial boundary value problems involving maxwell's equations in isotropic media," *Antennas and Propagation, IEEE Transactions on*, vol. 14, no. 3, pp. 302–307, May 1966.

[2] A. Taflove and S. C. Hagness, *Computational electrodynamics : the finite-difference time-domain method*, 3rd ed. Boston: Artech House, 2005.

[3] J. A. Roden and S. Gedney, "Convolutional PML (CPML): An efficient FDTD implementation of the CFS-PML for arbitrary media," *Microwave and Optical Technology Letters*, vol. 27, no. 5, pp. 334–339, 2000.

[4] W. C. Chew and W. H. Weedon, "A 3D perfectly matched medium from modified maxwell's equations with stretched coordinates," *IEEE Microwave and Guided Wave Letters*, vol. 7, no. 13, pp. 599–604, 1994.

[5] C. Rappaport, "Perfectly matched absorbing boundary conditions based on anisotropic lossy mapping of space," *Microwave and Guided Wave Letters, IEEE*, vol. 5, no. 3, pp. 90–92, 1995.

[6] R. J. Luebbers, "A frequency-dependent finite-difference time-domain formulation for transient propagation in plasma," *Antennas and Propagation, IEEE Transactions on*, vol. 39, no. 1, pp. 29–34, 1991.

[7] I. Giannakis and A. Giannopoulos, "Time-synchronized convolutional perfectly matched layer for improved absorbing performance in fdtd," *IEEE Antennas and Wireless Propagation Letters*, vol. 14, pp. 690–693, 2015.

[8] D. Correia and J.-M. Jin, "On the development of a higher-order PML," *Antennas and Propagation, IEEE Transactions on*, vol. 53, no. 12, pp. 4157–4163, 2005.

[9] ——, "Performance of regular PML, CFS-PML, and second-order PML for waveguide problems," *Microwave and Optical Technology Letters*, vol. 48, pp. 2121–2126, 2006.

[10] S. Gedney and B. Zhao, "An Auxiliary Differential Equation Formulation for the Complex-Frequency Shifted PML," *Antennas and Propagation, IEEE Transactions on*, vol. 58, no. 3, pp. 838–847, 2010.

[11] A. Giannopoulos, "Unsplit Implementation of Higher Order PMLs," *Antennas and Propagation, IEEE Transactions on*, vol. 60, no. 3, pp. 1479–1485, 2012.

[12] N. Feng and J. Li, "Novel and efficient FDTD implementation of higher-order perfectly matched layer based on ADE method," *Journal of Computational Physics*, vol. 232, no. 1, pp. 318–326, Jan. 2013.

[13] N. Feng, J. Li, and X. Zhao, "Efficient fdtd implementations of the higher-order pml using dsp techniques for arbitrary media," *IEEE Transactions on Antennas and Propagation*, vol. 61, no. 5, pp. 2623–2629, May 2013.
[14] J. A. Roden, J. Skinner, and S. Johns, "Effectiveness of a second order CPML absorbing boundary condition within the periodic FDTD method," *Antennas and Propagation Society International Symposium, 2009. APSURSI '09. IEEE*, pp. 1–4, 2009.
[15] M. Kuzuoglu and R. Mittra, "Frequency dependence of the constitutive parameters of causal perfectly matched anisotropic absorbers," *Microwave and Guided Wave Letters, IEEE*, vol. 6, no. 12, pp. 447–449, Dec. 1996.
[16] W. R. Inc., *Mathematica, Version 12.0*. Wolfram Research, Inc., 2019, champaign, IL. [Online]. Available: https://www.wolfram.com/mathematica
[17] J.-P. Bérenger, *Perfectly Matched Layer (PML) for Computational Electromagnetics*, ser. Synthesis Lectures on Computational Electromagnetics, J.-P. Bérenger, Ed. Morgan & Claypool, 2007.
[18] S. Gedney, "An anisotropic perfectly matched layer-absorbing medium for the truncation of FDTD lattices," *IEEE Transactions On Antennas and Propagation*, vol. 44, no. 12, pp. 1630–1639, 1996.
[19] A. Giannopoulos, "An Improved New Implementation of Complex Frequency Shifted PML for the FDTD Method," *Antennas and Propagation, IEEE Transactions on*, vol. 56, no. 9, pp. 2995–3000, Sep. 2008.

Antonios Giannopoulos received a B.Sc. (1991) in Geology from the Aristotle University of Thessaloniki, Greece and a D.Phil. (1997) in Electronics from The University of York, UK. He is currently a Reader and the Director of the Civil and Environmental Engineering Discipline in the School of Engineering, The University of Edinburgh, Edinburgh, U.K.. His research interests include computational electromagnetics and in particular the application of the FDTD method on the numerical modelling of ground penetrating radar. In addition, he works on the development and application of advanced radar and geophysical techniques for infrastructure sensing applications. He created gprMax, a freely available FDTD simulator, and he is directing its continuous development and enhancement. He was the General Chair of the 9th International Workshop on Advanced Ground Penetrating Radar, Edinburgh, 2017. He is a member of SEG and EAGE.